Moisture adsorption in glass wool products

LAURENT MARMORET[a,*], FLORENCE COLLET[b] AND HASSEN BEJI[a]

[a]*Université de Picardie Jules Verne - Laboratoire des Technologies Innovantes - Equipe Phénomènes de Transfert et Construction Durable, IUT Génie Civil – Avenue des facultés, le bailly – 80025 Amiens – France*
Tel : 33.2.22.53.40.09, Fax : 33.2.22.53.95.71
[b]*Université Européenne de Bretagne, Laboratoire de Génie Civil et Génie Mécanique, Equipe Matériaux Thermo Rhéologie IUT Génie Civil – 3, rue du Clos Courtel, BP 90422, 35704 Rennes France*

Received: April 19, 2010. Accepted: October 4, 2010.

Two glass wool insulating materials are studied. After describing the microscopic and macroscopic structure of the wool, the investigations are concentrated on water vapour sorption isotherm. The aim of this study is to calculate the values of parameters obtained by the regression of water sorption experimental data using Brunauer, Emmett and Teller (BET) and Guggenheim, Anderson and de Boer (GAB) and Three Sorption Stages (TSS) isotherms. We have chosen these isotherms because of their complementarity's range of relative pressures regression. BET isotherm can be applied for data until 0.4 even though GAB isotherm can be fitted until 0.84 and TSS one can be used on the whole range of relative pressures. Usually, new parameters are calculated independently for each (BET, GAB or TSS) model. There after, these values obtained from different models are compared. We have used this method in a first time. In a second time, another method is proposed: parameters are not independently calculated but values of the two parameters (monolayer and the energy constants) determined with the BET model are retained and used in the GAB model. So, we fit the experimental data with the BET values and a new additional constant, denoted k. Thereafter, GAB parameters are completed in TSS model by introducing a new constant, called h* to fit the whole range of relative pressures.

Keywords: Insulating material, mineral wool, glass fiber, adsorption isotherm, BET model, GAB model, TSS model.

*Corresponding author: laurent.marmoret@u-picardie.fr

1 INTRODUCTION

Mineral wool based materials are frequently used in the form of thermal insulation boards. This porous insulation material may be submitted to heat conduction, heat convection due to air motion, radiative heat flux among internal surfaces, moisture diffusion due to water vapour concentration gradients, water vapour convection due to air motion and phase transformation. The main processes involved with the accumulation of moisture within the insulation are either adsorption or condensation. Moisture accumulation due to adsorption occurs at the molecular level; i.e. mono-layers of water vapor molecules collected on the surfaces of glass-fibers [1]. This sorption process is often accompanied by thermal energy exchange that can alter the local temperatures significantly inside the material [2,3]. Energy is also released during the adsorption process as the molecules of water vapor become bound to the glass-fiber surfaces. Although the amount of moisture accumulation through adsorption is usually much smaller than that for condensation, the heat of adsorption can be up to four times as high as the heat of vaporization. Due to the complexity of the interaction among these physical effects, it is often difficult to analyze the data obtained from field measurements [4]. Adsorption phenomena can be described using the relationship between the equilibrium pressure of the gas and the amount adsorbed at constant temperature, known as adsorption isotherm. The Brunauer–Emmett–Teller (BET) model [5,6] and the extension known as Guggenheim–Anderson–de Boer (GAB) model [7,8] are widely used. The GAB model becomes inadequate at relative pressures higher than 80 to 90%. Thereafter, a new stage becomes available for the sorbate molecules (which are true liquid-like properties): the Three Sorption Stage (TSS) [9].

In this paper, two mineral insulating materials manufactured by Isover are studied. In a first part, we describe the microscopic and macroscopic structure of the wool to assess materials properties. In a second part, water vapour sorption isotherm is studied to analyse the moisture adsorption phenomena. The sorption curves are fitted with BET, GAB and TSS models and values of the parameters are compared.

2 MATERIALS AND SAMPLES

We study two different glass wools, denoted L1 and L2, sold in the form of panels. They are both intended for the insulation of roofs. To product the wool, glass fibers are interconnected by a synthetic binder and by additives such as anti-mould admixtures. According to the manufacturer, they are both generally made for 90% of glass fiber and for 10% of formo-phenolic binders.

2.1 Microscopic structure and chemical analysis

Scanning Electron Microscopy (SEM) shows heterogeneity of the geometry of fibers and the random distribution of fibers (fig. 1). Wools are composed

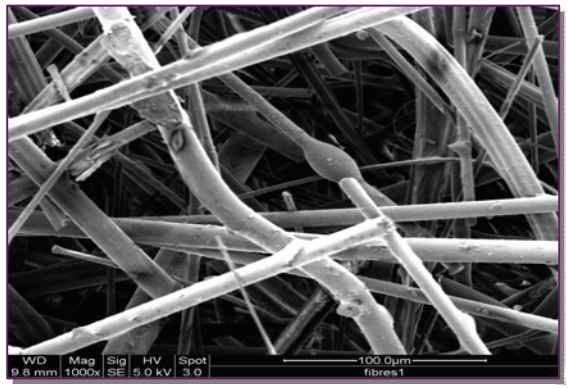

FIGURE 1
Scanning Electron Microscopy of L1.

by fibres of 14 µm diameter which is a rather significant dimension with respect to the wools standards. Binders appear in the form of droplets and clusters. We have observed that the binder is distributed fairly regularly along the fibers. The average thickness of the binder is estimated at about 500 nm. Coupling the SEM with the EDX detector, the chemical composition of fibers and binder is analysed. The L1 and L2 fibers are made, in a large proportion, of recycled glass and its chemical composition is classified into the classic E-type [10]. According to the type of wool, the contents of silicon (Si), sodium (Na), calcium (Ca) and potassium (K) are greatly different [11]. Moreover, the binder of glass wool noted L1 is distinguished by the presence of magnesium (Mg), and sulfur (S) is found in the binder in L2.

The Thermo-Gravimetric Analysis (TGA) has been used to determine the temperature which caused the degradation of the glass wools binders. The global amount of mass change can be also calculated. But, this technical method does not distinguish between free water and bound water [12] of the water contents inside the amount of mass change. Both L1 and L2 thermograms (fig. 2) show two-step combustion in air of the coated glass fibers. The first step is due to evaporation of the adsorbed moisture (from 100 up to 210°C) and the second one can be assigned to the decomposition of binders (210–550°C). When samples are immersed in liquid water for 24 h at a temperature of 20 $\pm$ 1°C, L1 looses approximately 64% of water even though L2 looses almost 70% (fig. 2) during the first step. Moreover, we observe in fig. 2 that after 200°C, mass change of L2 (almost 1%) is less than mass change of L1 (almost 4%). This difference can be explained by a dilution of a part of the binder in liquid water. This part of the binder can be evaporated before the decomposition of binders (210–550°C) and explained the least mass change of L2 than L1 during this period in fig. 2. Zinck and al. [13] have also proposed this hypothesis to explain the ageing of the glass fiber.

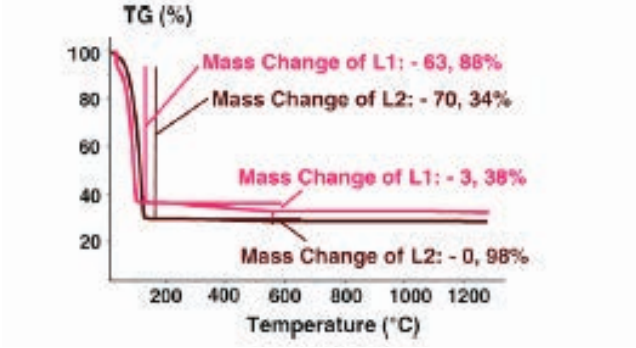

FIGURE 2
TGA thermograms of L1 and L2 samples immersed in liquid water during 24 h [11].

TABLE 1
Structural characteristics of the wools.

	Average diameter of the fibre ϕ [μm]	Volumetric Surface S_V [μm^{-1}]	Porosity [%]	Density [$g.cm^{-3}$]
Glass wool L1	13	0,31	96,96	0,079
Glass wool L2	14	0,29	95,42	0,119

Their conclusion is the main cause of ageing is due to the binders and the alteration of glass constituting fibers comes much later. During the adsorption phenomena, the surface of contact with the moisture is the binder. But the binder can de diluted if liquid water appears in the porous structure of the wool.

2.2 Macroscopic analysis

The structure of wools was characterized by morphological parameters such as porosity, density and volumetric surface. Total porosity ε is calculated with the apparent bulk density of the sample in a dry state and with the density of its solid matrix constituted of E-type glass. Volumetric surface S_V expresses the degree of division of the solid phase. Its value is obtained theoretically by carrying out the relationship between developed surface and the unit of volume of matter constituting the solid phase. For fibrous insulators, according to the work of Klarsfeld and Al. [14], volumetric surface can be calculated by: $S_V = 4 / \phi$ where ϕ represents the average diameter of fibre. The wools L1 and L2 having densities higher than 20 $kg.m^{-3}$ and porosities near 96% (table 1), they can be classified in the category of heavy insulators. The insulators used in building industry come from this category in general.

3 POROUS STRUCTURE ANALYSIS FROM SORPTION ISOTHERMS

As, our wools are very porous ($\varepsilon > 95\%$) and have an important volumetric surface, the surface of contact between the absorbate and the absorbent is significant. The behaviour of the adsorbate on the adsorbent can lead to a monolayer adsorption, where all the adsorbed molecules are in contact with the surface of the adsorbent, or to a multilayer adsorption in which the adsorption space accommodates more than one layer of the adsorbate.

3.1 Sorption models theory

In the lower half of the range of relative pressures ($0.05 < \varphi < 0.35 - 0.40$), molecules are strongly sorbed in a monomolecular layer (First stage, Fig. 2). The amount of adsorbate needed to cover the surface with a complete monolayer of molecules is known as monolayer capacity and the surface area of the adsorbent may be calculated from the monolayer capacity. The Brunauer, Emmett and Teller (BET) sorption equation represents a fundamental model in the interpretation of this range of relative pressures. The success of the BET model is more qualitative than quantitative because it can be performed only over the lower half of the range of relative pressures ($0.05 < \varphi < 0.4$). This inability to fit the experimental data over the whole range of the relative pressures has induced that the principal application of the BET equation has been the estimation of the surface area. Only two constants characterize the BET isotherm equation, namely ω_m, the monolayer sorption capacity and C, a parameter related to the energy difference of the sorbate molecules in the first layer and in the other 'liquid-like' layers (or in the pure liquid).

With increasing relative pressures, molecules are sorbed in multimolecular layers (Second stage). In almost every case, the amount sorbed by the sorbent is less than that predicted by the BET isotherm [5,6]. By postulating that the state of the sorbate molecules in the second and higher layers is the same but different from that in liquid-like state, Guggenheim, Anderson and de Boer

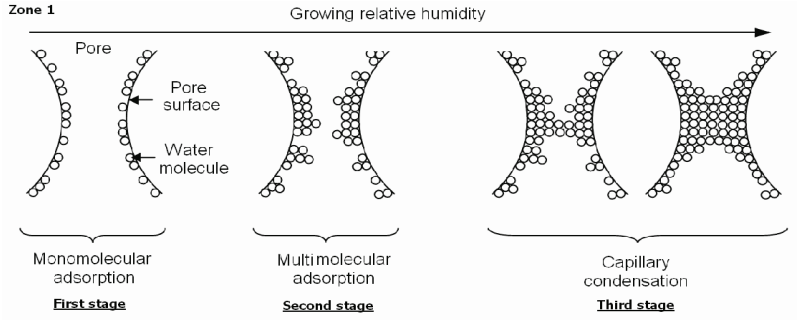

FIGURE 3
Physisorption.

TABLE 2
Model equations fitted to the experimental sorption data.

Model	Mathematical expression	
BET [5,6]	$\frac{w}{w_m} = \frac{C.\varphi}{(1-\varphi)(1-\varphi+C\varphi)}$	(1)
GAB [7,8]	$\frac{w}{w_m} = \frac{C.k.\varphi}{(1-k\varphi)(1-k\varphi+Ck\varphi)}$	(2)
TSS [9]	$\frac{w}{w_m} = \frac{C.H(\varphi).H'(\varphi).k.\varphi}{(1-k\varphi)(1-k\varphi+Ck\varphi)}$	(3)

(GAB) [7,8] introduce a second well differentiated sorption stage for the sorbate molecules. GAB model can reproduce the experimental data up to $\varphi \leq 0.9$. This isotherm necessarily contains a third constant k, which quantifies the difference between the standard chemical potentials of the molecules in the second sorption stage and in the pure liquid state. In most practical cases, k is less than the unity because, a lower sorption than allowed by the BET model is predicted for relative pressures greater than 40%. Lastly, capillary condensation appears at higher relative pressures (Third stage). A refinement of the GAB model is to introduce a third stage into the formulation and thereby derive a Three Sorption Stage (TSS) isotherm. As BET and GAB method, the TSS isotherm will be deduced by a statistical method describing the sorption curve. Theoretical foundations are described by Timmermann [9]. TSS isotherm retains the mathematical form of previous isotherms and integrates two correction relations H(φ) and H'(φ) which depend on a new constant h*. These relations become important only at high relative activities of the sorbate.

The different mathematical expressions chosen to fit the experimental sorption data are:

ω is the experimental moisture content adsorbed on the sample at relative pressure φ P / P_o where P is the pressure of adsorbate and P_o is the saturated vapour pressure of adsorbate. ω_m is the moisture content when the adsorbent surface area is covered with a complete monomolecular layer. In the GAB model, k is the GAB constant related to the properties of multilayer water molecules with respect to the bulk liquid. The parameters C can be correlated with temperature, using the following Arrhenius-type equations: $C = C_o \exp\left(\frac{E_1 - E_m}{R.T}\right)$ where C_0 is pre-exponential factors, E_1, E_m and E_L (kJ mol^{-1}) aremolar sorption enthalpies, respectively, of the mono-molecular layer, of the multilayers covering the mono-layer and of the bulk liquid water. R and T are the universal gas constant and the absolute temperature.

The function H(φ) and H'(φ) are defined by:

$$H(\varphi) = 1 + \frac{1-k}{k} . \frac{(k.\varphi)^{h^*}}{1-\varphi} \tag{4}$$

$$H'(\varphi) = 1 + \frac{H(\varphi)-1}{H(\varphi)} . \frac{(1-k.\varphi)}{1-\varphi} \left[h^* + (1-h^*).\varphi \right] \tag{5}$$

Two values of h* (h* = 1 and h* $\rightarrow \infty$) are interesting:

- If h* $\rightarrow \infty$, H(φ) and H'(φ) $\rightarrow$ 1, eq (3) transforms into the GAB model (eq. 2).
- If h* = 1, H(φ) and H'(φ) $\rightarrow$ H'(φ) $\rightarrow \frac{1-k.\varphi}{1-\varphi}$, eq (3) transforms into the BET model (eq. 1).

3.2 Experimental results and discussion

The measurements [15] of adsorption isotherms were performed in laboratory conditions at 23 $\pm$ 1°C. The samples were placed in desiccators with different solutions (table 4) to simulate different values of relative pressures.

The initial state was dry material (m_o) after maintained samples in an oven at 80°C. The mass of samples was measured until the steady state value of the mass was achieved (m_w). Then, the equilibrium moisture content by mass (ω) was calculated according by gravimetric method:

$$\omega = \frac{m_w - m_O}{m_O} \, [\text{kg.kg}^{-1}] \tag{6}$$

The volumetric water content (θ) can be calculated with $\theta_l = (\rho_l / \rho_o), \omega$ where ρ_l and ρ_o are densities of water and material respectively. The experimental results on the equilibrium volumetric moisture content against relative pressures are given in Fig. 5. According to IUPAC classification [15], these sorption curves are classified as type II corresponding to non-porous or macroporous media. The curves obtained for the two wools are quite the

TABLE 3
Saturated salt solutions.

Saturated salt solutions		**Relative pressures (%) at 23°C**
Potassium hydroxide	KOH	8
Sodium fluoride	NaF	57
Sodium chloride	NaCl	75
Potassium chloride	KCl	84
Potassium sulfate	K2SO4	97

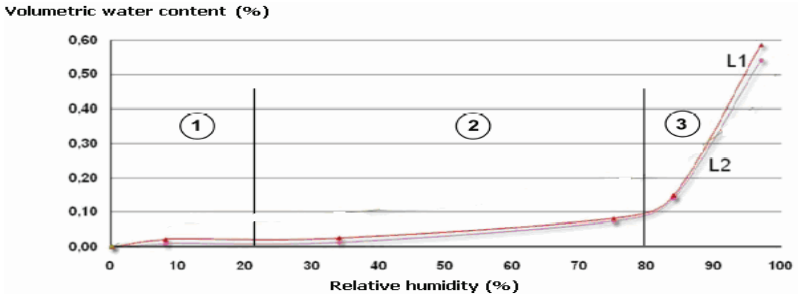

FIGURE 4
Sorption isotherm for glass wool (L1 and L2).

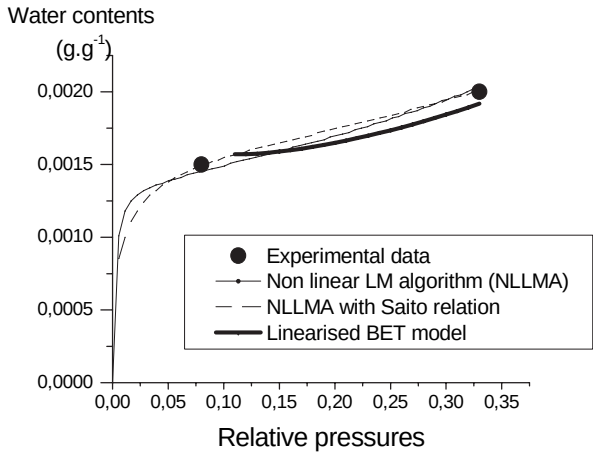

FIGURE 5
BET model for L1.

same but we notice that L1 is a little more hygroscopic than L2. Three clearly defined regions can be distinguished. For $0 < \varphi < 0.8$, in the adsorptionally bound moisture region (with mono on the part ① and multi-molecular layer on part ②), the amount of water adsorbed is very small. Volumetric water content doesn't exceed 0.1. In the capillary bound moisture region ($\varphi > 0.8$), the increase of volumetric water content is very important. For example, at $\varphi = 0.90$, volumetric moisture content is 0.30 for L2 and 0.34 for L1. The water content difference cannot be only assigned to the experimental error which doesn't exceed 5%.

Ya and al. [16] have investigated specimens of glass fibers products as well as mineral wool manufactured by Isover (Netherland, Finland) and Paroc (Finland, Poland, Lithuania). Mean diameter of the glass fiber was $5\,\mu$m. The investigated products represent a material consisting of fine glass fibers interconnected by a synthetic binder. They have compared water content sorbed in

TABLE 4
Effect of Admixture on volumetric water content for $\varphi = 75\%$.

	Rockwool mineral wools [17]			Our mineral wools	
	With hydrophobic admixtures	**with hydrophilic admixtures**	**without admixtures**	**L1**	**L2**
Density (kg.m^{-3})	110	120	90	119	79
Volumetric water content	0.059%	0.103%	0.096%	0.084%	0.074%

glass fiber and in mineral wool. The investigated glass fiber product obtain a higher hygroscopy than the mineral wool one. Water content can be 5 or 10 times higher for the glass fiber boards than for the mineral wool of the same density. However, they assign the variation of water content to the binder content by testing different binders on a same glass fiber. Another interesting work [17] studies the effect of adding additives, such as anti-mould admixtures in the binder of mineral wools. They compare the behaviour of mineral wools manufactured by Rockwool with hydrophobic, with hydropholic admixtures and without any admixture. In the adsorption curve, we draw out the volumetric water content of each mineral wool for a relative pressure equal to 75% (at the end of the adsorptionally bound moisture region). A distinct result is obtained (table 4) with hydrophobic and with hydrophilic agent for quite the same density of material. Their effect on adsorption phenomena is clear but we don't have this information for our wools.

3.3 Model results and discussion

The following recipe was adopted to determine the values of the parameters C, ω_m, k, h*, H(φ) and H'(φ) with Eqs. (1), (2) and (3) of the BET, GAB and TSS models.

3.3.1 BET Isotherm

Usually, the analysis of adsorption data in the BET range uses the linearised form of eq. (7) to determine the two characteristics constants (C_B and ω_{mB}):

$$F_{BET} \equiv \frac{\varphi}{(1-\varphi).\omega} = \frac{1}{C_B.\omega_{mB}} + \frac{C_B - 1}{C_B.\omega_{mB}}.\varphi \qquad (7)$$

By plotting the experimental data in the form F_{BET} versus φ a straight line is obtained. The straight line intercept $1/C_B.\omega_{mB}$ and slope $(C_B - 1)/C_B.\omega_{mB}$ can be easily evaluated. From the two equations for slope and intercept, the value of C_B and ω_{mB} are obtained separately. But BET isotherm with the linearised form overestimates values of C [18]. This is caused by the rapid increase of adsorption at low relative pressures which results in a distinct 'knee' on the isotherm. For an unknown porous sample the presence of

micropores (according to IUPAC definition pores with sizes smaller than 2 nm) can not be excluded. The adsorption isotherm will have the shape in-between isotherm types I and IV, the presence of micropores has to be checked and taken into account. We have to take the micropores into account because sorption curves of L1 and L2 are classified as type II (cf § II.2). Saito and al. [19] recently developed relations for average potential energy profiles of adsorbate in cylindrical pores of oxide adsorbents and used them to obtain the dependence of pore radius and relative pressure on pore filling by adsorbate. So by using Saito relations, it's possible to describe the combined adsorption in both micropores and macropores with the modified BET adsorption equation:

$$\omega = V_{mi}^{0} + \frac{\omega_m.C.\varphi}{(1-\varphi)(1-\varphi+C\varphi)} \tag{8}$$

Where V_{mi}^{0} represents the net volume of adsorbate which fills the micropores.

An alternative method of the linearised form (eq. 7) the non linear Levenberg-Marquardt algorithm have been used to determine the three isotherm parameters V_{mi}^{0}, C_B and ω_{mB},. Table 5 show results from different method. Whatever the method, the monomolecular moisture content ω_{mB} is always greater for L2 than for L1. C_B value is negative with linearised form (eq. 7) and tends towards an infinite value with BET method (eq. 1). ω_{mB} value for linearised form is smaller than with BET method for the two wools. By using Saito relations (eq. 8), regression coefficient (R^2) is better and the net volume of adsorbate which fills the micropores (V_{mi}^{0}) is known. For C_B, we have written in table 5 a value equal to 60 but a greater value can be incorporated because no effect on the fit is observed.

Figure 6 and 7 show water contents against relative pressures for L1 and L2 wools respectively. We can't obtain a good fit for relative pressures under 0.1 with linearised form.

TABLE 5
BET parameters for L1 and L2.

	Linearised BET model		**Non linear Levenberg-Marquardt algorithm (NLLMA)**			
			BET method (eq. 1)		**BET model with Saito parameters (eq. 8)**	
	L1	**L2**	**L1**	**L2**	**L1**	**L2**
V_{mi}^{0} (kg.kg^{-1})	–	–	–	–	0.00061	0.00060
C_B	−77	−77	500	∞	60	60
ω_{mB} (kg.kg^{-1})	0.00125	0.00148	0.00142	0.00157	0.00097	0.00123
R^2			0.973	0.762	0.999	0.806

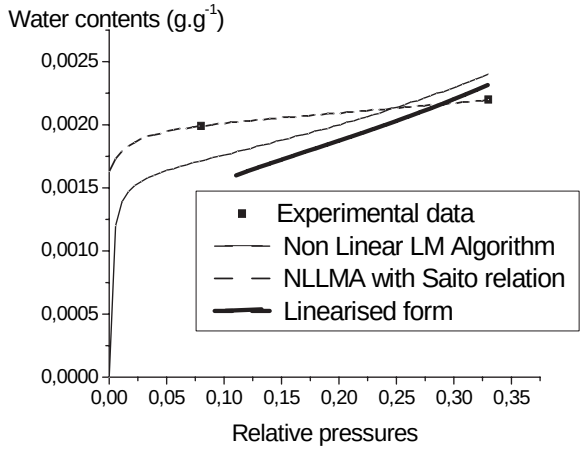

FIGURE 6
BET model for L2.

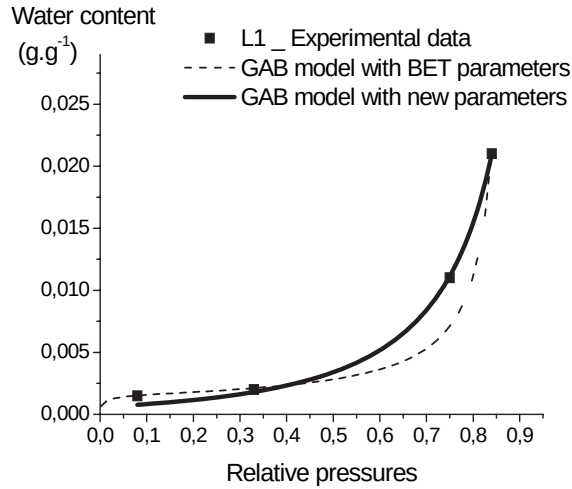

FIGURE 7
GAB model for L1
(regression only with NLLMA + Saito relations).

3.3.2 GAB Isotherm

We have only used the Saito relations with the non linear Levenberg-Marquardt algorithm (NLLMA) to calculate GAB constants (V^0_{mi}, C_B, ω_m and k) in the range of relative pressures below $\varphi_{max} = 0.90$. We want to compare results from two methods. The first one denoted 'GAB model with BET parameters' in figure 8 and 9 retain the BET values (with Saito relation) and a new constant k is added. The second method denoted 'GAB model with

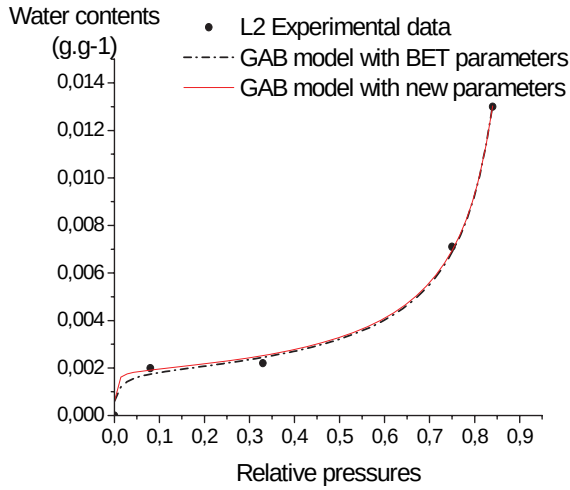

FIGURE 8
GAB model for L2
(regression only with NLLMA + Saito relations).

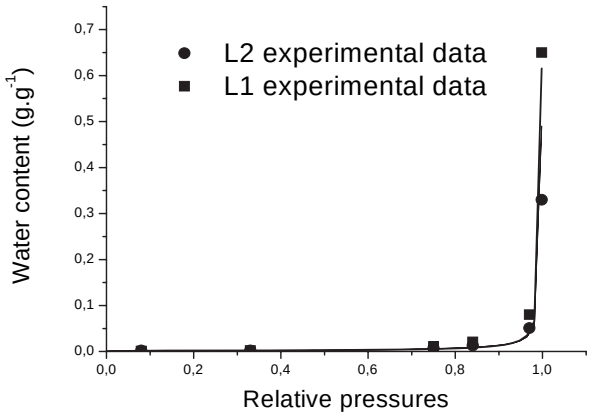

FIGURE 9
TSS model for L1 and L2.

new parameters' doesn't use BET values but determines new values for V_{mi}^{0}, C_B, ω_m and k. This second method is the ordinary one because it allows a comparison of the results obtained with BET and GAB isotherm. For low relative pressures, the first method provides a better fit. But for the great relative pressures, the opposite interpretation can be done. That's why we observe for the wool L1 a better regression coefficient (table 6) for the second method than for the first one. For L2, the only difference appears for the low relative pressures. So the interest of using new parameters is not as obvious as we can think before this comparison.

TABLE 6
GAB parameters for L1 and L2.

Non linear Levenberg-Marquardt algorithm (NLLMA) using Saito relations				
	With BET parameters		With new parameters	
	L1	L2	L1	L2
V^0_{mi} (kg.kg^{-1})	0.00061	0.00060	0.0006	0.0006
C_B	60	60	0.42	257
ω_{mB} (kg.kg^{-1})	0.00097	0.00123	0.00473	0.00126
k	1.135	1.073	1.15	1.070
R^2	0.939	0.995	0.997	0.995

We observed in table 6 best fit is obtained for a constant k near but greater than the unity. It is not conform to the fact related in the literature. We discuss of this point in the § II.3.4.

As Timmermann [9], we have observed that ω_m values with BET isotherm (denoted $\omega_{m\,(BET)}$) are smaller ($\omega_{m(BET)} < \omega_{m(GAB)}$) than ω_m values with GAB isotherm (denoted $\omega_{m\,(GAB)}$). For the energy constant C_B, we have also obtained the same inequalities than Timmermann: $C_{B(BET)} > C_{B(GAB)}$ but variations are very small. Another interesting point concerned constant k. Timmermann [21] says that k is always less than the unity for food. Only one case has been found for $k > 1$ in the literature. It corresponds to the system NaDNA-H_2O studied by Gascoyne and Pethig [22]. The constant k introduce the difference of the free enthalpy (standard energy potential) of the sorbate molecules in the two states: the pure liquid and the second sorption stage corresponding to the layer above the first layer. The constant k determines the profile at the higher activity range regulating the upswing after the plateau following the 'knee' at the medium range. A too high k-value determines an upward curvature in the GAB plots as in the BET plots. As we obtain $k > 1$ for the two wools, with the integration of k in eq. (2), the sorption will become infinite at a value of the relative pressure less than unity denoting instability of the system. So, we can proposes two explanations: firstly, the larger the number of experimental points and the better their accuracy so we need more experimental data to verify our result and secondly, values of k less than unity is observed for food but it can be different for mineral wool.

3.3.3 TSS Isotherm

TSS isotherm is used to fit experimental data in the whole range of the relative pressures. A new characteristic h* is introduced in the relations $H(\varphi)$ and $H'(\varphi)$. As we conclude before that using new parameters bring not an obvious interest, we use to fit the TSS isotherm the alues obtained

for GAB regression (k) and BET regression (V^0_{mi}, C_B and ω_m). A good accuracy of the fitting can be admitted with the regression coefficient (R^2). Al-Muhtaseb and al. [20] consider a good fitting if difference between experimental and predicted values are lower than 10%. Constant h* ranges between 0 and ∞. With the increase of h*, the effect of the function H and H' becomes more and more restricted to the region of highest values of relative pressures φ. Value of h* for L1 ($h^* = 11.1$) is conform to Timmermann results [9] for interaction gas/solids (between 8 to 15). For L2, h* is near the unity so, as we have mentioned in § II.1, TSS model can be transformed into the BET model.

3.3.4 Solid surface area

Once the monolayer moisture content (ω_m) is known, the solid surface area (S in $m^2\ g^{-1}$) of the samples can be determined:

$$S = \sigma_m.N.\frac{\omega_m}{M} \tag{9}$$

where σ_m is the area of a water molecule ($1.06\ 10^{-19}\ m^2$ molecule^{-1}), N is the Avogadro's number ($6.023\ 10^{26}$ molecules kg.mol^{-1}) and M is the molecular weight of water ($18\ g\ mol^{-1}$).

So, the specific surface area calculated from the BET value of monomolecular water content is $5\ m^2.g^{-1}$. Veiseh and al. [23] determine specific surface area of different fibrous insulation by an indirect test of fineness index based upon Darcy's law. The equipment utilized in this test is named Micronaire and they measure a fineness index: 3.0 and $5.0\ m^2.g^{-1}$. We can consider that our results are quite similar with L1 and L2.

TABLE 7
TSS parameters for L1 and L2.

	TSS model with Saito parameters (eq. 8)	
	L1	**L2**
h*	11,10	0.48
R^2	0.92	0.97

TABLE 8
Surface specific area for L1 and L2.

	L1	**L2**
ω_m ($g.g^{-1}$)	0.00097	0.00123
S ($m^2.g^{-1}$)	3.25	4.12

4 CONCLUSIONS

Water vapour sorption of two different glass wools is studied. These high porous materials are composed of E-type glass fibers which are interconnected by formo-phenolic binder. With thermo-gravimetric analysis (TGA) the importance of the binder in adsorption phenomena is showed. We have distinguished three regions of the sorption isotherm. Firstly, in the monomolecular layer (for the relative pressure range: humidity $0.05 < \varphi < 0.35 - 0.40$), we have determined, by using the BET model, two parameters, respectively for L1 and L2: the monomolecular water content (ω_m) is 9.7 and 12.3 10^{-4}kg.kg^{-1} and the specific surface area (S_m) is 3 and 4 m².g^{-1}. An improvement has been observed by the modified BET adsorption isotherm with Saito and Foley's expressions. By using Saito relation, we determine the net volume of adsorbate which fills the micropores to 6. 10^{-4} kg.kg^{-1}. Secondly, for the range of relative pressures below $\varphi_{max} = 0.90$, we obtain a constant k in the GAB model greater than the unity which have been rarely observed for adsorption isotherm. For relative pressure (φ) less than 80% (mono and multi molecular layers), the amount of water adsorbed is very small for L1 and L2. In the capillary bound moisture ($\varphi > 80\%$), the increase of water content is important. We have used the TSS model to fit the whole range of relative pressures. A good accuracy is obtained by using the values calculated before with BET and GAB regressions.

REFERENCES

[1] Tao Y.-X., Besant R. W. and Simonson C. J., Measurement of the heat of adsorption for a typical fibrous insulation, ASHRAE Trans. ∼98(2), 495–501 (1993).

[2] Vafai K. and Tien H. C., A numerical investigation of phase change effects in porous materials, Int. J. Heat/Mass Transfer 32, 1261–1277 (1989).

[3] Tao Y.-X., Besant R. W. and Rezkallah K. S., The transient thermal response of a glass-fiber insulation slab with hygroscopicity effects, Int. J. Heat Mass Transfer 35, 1155–1167 (1992).

[4] Hedlin C. P., Effect of moisture on thermal resistances of some insulations in a flat roof system under field-type conditions, ASTM STP 789, pp. 602–625 (1983).

[5] Brunauer, S., Emmett, P. H., Teller, E., 1938. Adsorption of gases in multimolecular layers, Journal of the American Chemical Society 60, 309.

[6] Iglesias, H. A., Chirife, J. BET monolayer values in dehydrated foods and food components. Lebensmittel-Wissenschaft + Technologie, 9, 107±113 (1976a).

[7] Van den Berg, C., Bruin, S., 1981. Water activity and its estimation in food systems: theoretical aspects. In: Rockland, L. B., Stewart, G. F. (Eds.), Water Activity: Influences on Food Quality. Academic Press, New York, pp. 1–61.

[8] Bizot, H. (1983). In R. Jowit. Using the GAB model to construct sorption isotherms, Physical Properties of Foods (pp. 43)54). London: Applied Science.

[9] Timmermann E. O, A BET- like three sorption stage isotherm, J. Chem. Soc. Faraday trans. 85(7), 1631–1645, 1989.

[10] H. Talbot. Analyse morphologique de fibres minérales d'isolation. PhD thesis, École Nationale Supérieure des Mines de Paris, 1993.

[11] Achchaq F., Djellab K., Marmoret L., Beji H., Hydric, morphological and thermo-physical characterization of glass wools: From macroscopic to microscopic approach, Construction and Building Materials, 23, 3214–3219 (2009).

[12] Wang W, Longxiang T, Baojun Q. Mechanical properties and morphological structures of short glass fiber reinforced PP/EPDM composite. Eur Polym J 39, 2129–2134. 2003.
[13] Zinck P., De la caractérisation micromécanique du vieillissement hydrothermique des interphases polyepoxyde – fibre de verre au comportement du composite unidirectionnel. Relation entre les échelles micro et macro, INSA Lyon, France, 1999.
[14] Klarsfeld S., Langlais C., Transferts de chaleur à travers les isolants fibreux en relation avec leur morphologie, Journée d'études du groupement universitaire de thermique, Transfert de chaleur dans les isolants fibreux, 6 mars 1985.
[15] International Union of Pure and Applied Chemistry. Reporting physisorption data for Gas/solid systems with special reference to the determination of surface area and porosity, Pure and Applied Chemistry, Vol. 57, N°4, pp 603–619, 1986.
[16] Ya I., Gnip S., Veyalis A., Kershulis V. I, Isotherms of water vapor sorption by light inorganic and polymer heat-insulating materials, Journal of Engeneering physics and thermophysics, Vol. 79, N°1, 2006.
[17] Jirickova M., Cerny R., Effect of hydrophilic admixture on moisture and heat transport and storage parameters of mineral wool, Construction and Building materials, 20, pp 425–434, 2006.
[18] Schneider P, Adsorption isotherm of microporous-mesoporous solids revisited, Applied Calatlysis A: General 129, pp 157–165, 1995.
[19] Saito A. and Foley H. C, AIChE J., 37, 429, 1991.
[20] Al-Muhtaseb A. H., McMinn W. A. M., T. R. A. Magee, Water sorption isotherms of starch powders Part 1: mathematical description of experimental data, Journal of Food Engineering 61, pp 297–307, 2004.
[21] Timmermann. E. O, Multilayer sorption parameters: BET or GAB values?, Colloids and surfaces A, 220, pp 235–260, 2003.
[22] Gascoyne P. R. C. and Pethig R., J. Chem. Soc. Faraday Trans., I, 73, 171, 1977.
[23] Veiseh S., Khodabandeh N., Hakkaki-Fard A., Mathematical models for thermal conductivity density relationship in fibrous thermal insulations for practical applications, Asian Journal of civil engineering (Building and housing) Vol. 10, N°2, pp 201–214, 2009.